HHS Public Access

Author manuscript

J Physiol. Author manuscript; available in PMC 2024 June 01.

Published in final edited form as:

J Physiol. 2023 June ; 601(12): 2371–2389. doi:10.1113/JP284552.

Exercise improves homeostasis of the intestinal epithelium by activation of apelin receptor-AMP-activated protein kinase signalling

Song Ah Chae[1], **Min Du**[1], **Jun Seok Son**[2,3,*], **Mei-Jun Zhu**[4,*]

[1]Nutrigenomics and Growth Biology Laboratory, Department of Animal Sciences, Washington State University, Pullman, WA 99164, USA

[2]Laboratory of Perinatal Kinesioepigenetics, Department of Obstetrics, Gynecology & Reproductive Sciences, University of Maryland School of Medicine, Baltimore, MD 21201, USA

[3]Department of Physiology, University of Maryland School of Medicine, Baltimore, MD 21201, USA

[4]School of Food Science, Washington State University, Pullman, WA 99164, USA

Abstract

Intestinal remodeling is dynamically regulated by energy metabolism. Exercise is beneficial for gut health, but the specific mechanisms remain poorly understood. Both intestine-specific apelin receptor (APJ) knockdown (KD) and wild-type male mice were randomly divided into two subgroups with/without exercise to obtain four groups: WT, WT with exercise, APJ KD, and APJ KD with exercise. Animals in exercise groups were subjected to daily treadmill exercise for 3 weeks. Duodenum was collected at 48h after the last bout of exercise. AMP-activated protein kinase (AMPK) α1 KD and wild-type mice were also utilized for investigating the mediatory role of AMPK on exercise-induced duodenal epithelial development. AMPK and peroxisome proliferator-activated receptor γ coactivator-1 α (PGC-1 α) were upregulated by exercise via APJ activation in the intestinal duodenum. Correspondingly, exercise induced permissive histone modifications in the PR domain containing 16 (PRDM16) promoter to activate its expression, which was dependent on APJ activation. In agreement, exercise elevated the expression of mitochondrial oxidative markers. The expression of intestinal epithelial markers was downregulated due to AMPK deficiency, and AMPK signaling facilitated epithelial renewal. These data demonstrate that exercise-induced activation of APJ-AMPK axis facilitates the homeostasis of the intestinal duodenal epithelium.

Graphical Abstract

[*]**To whom correspondence should be addressed: Jun Seok Son, Ph.D.**, Department of Physiology, Department of Obstetrics, Gynecology and Reproductive Sciences, University of Maryland School of Medicine, Baltimore, MD 21201, USA, Phone: (410)706-3031, junseok.son@som.umaryland.edu; **Mei-Jun Zhu, Ph.D.**, School of Food Science, Washington State University, Pullman, WA 99164, USA, Phone: (509)335-4016, meijun.zhu@wsu.edu.

Author contributions. S.A.C. designed, performed experiments, analyzed, and interpreted the data, and wrote the manuscript. M.D., J.S.S., and M-J.Z. designed, interpreted the data, and edited the manuscript.

Competing interests. The authors declare no competing interests.

Exercise training increases expression of apelin in muscle and the circulating apelin level. Exercise-induced apelin-APJ signaling enhances villus and crypt structure of the small intestine (duodenum) through the activation of AMPK and stimulation of mitochondrial biogenesis. Of note, exercise program induces histone modifications for PRDM16 expression, which enhances mitochondrial oxidative metabolism, thereby improving intestinal epithelial homeostasis.

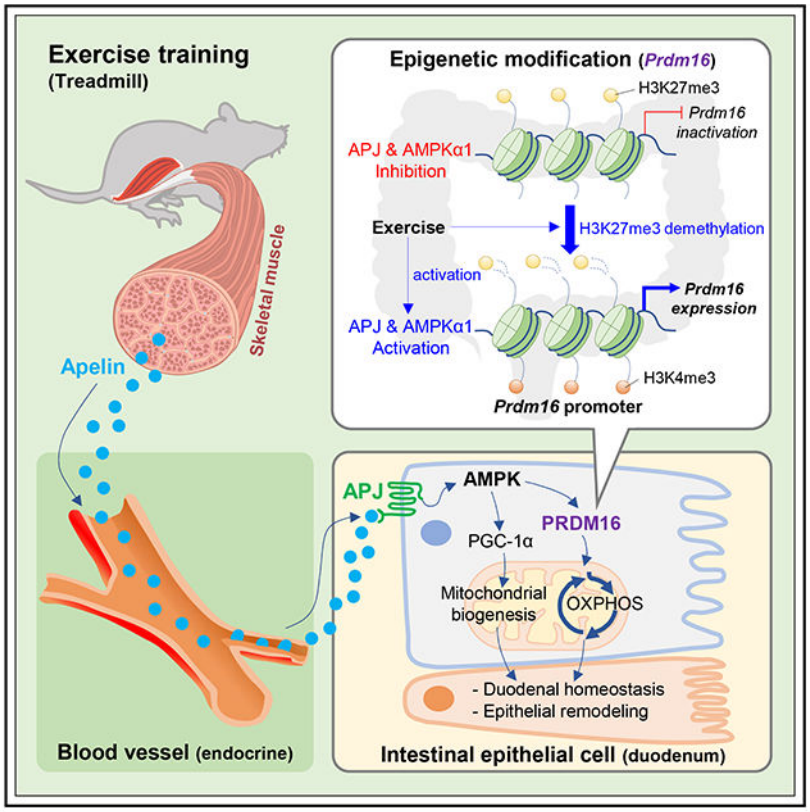

One-sentence summary:

Exercise-induced APJ-AMPK axis upregulated the expression of PGC-1α and PRDM16 to improve homeostasis of intestinal epithelium.

Keywords

AMPK; APJ; duodenum; exercise; mitochondrial oxidation; PRDM16

Introduction

Small intestinal epithelium, made up of villi and crypts, is mainly responsible for absorption of nutrients including carbohydrates, fats, protein, vitamins, and water, while blocking the passage of harmful compounds and potential pathogens. Intestinal stem cells (ISCs) produce transit-amplifying (TA) progenitor cells, which migrate from the crypt to the villus while differentiating into absorptive or secretory epithelial cells (Snippert et al., 2010; Kurokawa et al., 2020). Intestinal epithelium self-renews every few days, thus, high levels

of intestinal stem/progenitor cell proliferation is required (Blanpain et al., 2007). In addition, oxidative metabolic transition occurs in epithelial cells during differentiation (Folmes et al., 2012). Although glycolysis is a dominant source of energy for ISC self-renewal, fatty acid oxidation (FAO) enhances stem cell function (Mihaylova et al., 2018). Moreover, as an energy demanding tissue, intestinal epithelium is vulnerable to nutritional deprivation and high-fat diet, which negatively impacts ISC proliferation and differentiation (Beyaz et al., 2016; Mihaylova et al., 2018). Up to now, the roles of metabolic transition and FAO in regulating ISC proliferation and subsequent differentiation remain poorly defined.

Apelin, a peptide hormone regulates energy metabolism in multi-organs (Bertrand et al., 2015), which exerts its biological effects through its receptor APJ, a G protein-coupled receptor (GPCR) (O'Carroll et al., 2013). Activation of Apelin/APJ signaling promotes mitochondrial biogenesis and oxidative metabolism in brown fat and skeletal muscle (Son et al., 2020a; Son et al., 2020b). APJ stimulates the transcription of peroxisome proliferator-activated receptor γ coactivator-1α (PGC-1α) to activate mitochondrial biogenesis in brown fat (Than et al., 2015; Hu et al., 2016). In addition, APJ regulates the proliferation and differentiation of stem/progenitor cells, including hematopoietic and cardiac stem cells (Ando et al., 2017; Hou et al., 2017). As an exerkine, APJ signaling is dramatically enhanced by exercise (Zhang et al., 2006; Ji et al., 2017), and exercise training is considered as a therapy for improving the properties of hematopoietic, neural, epithelial, and mesenchymal stem cells (Lin et al., 2013).

Excitingly, APJ is highly expressed in intestinal epithelial cells (Wang et al., 2004) but its roles in epithelial homeostasis remains to be defined. Here, we show that APJ signaling mediates the beneficial effects of exercise on epithelial homeostasis. Exercise enhances mitochondrial biogenesis and FAO by activating APJ signaling. We further found that exercise-mediated APJ activates AMPK phosphorylation, which induces the expression of PGC-1α and PRDM16, known to stimulate mitochondrial biogenesis and FAO. Together, these results demonstrate the possible therapeutic role of exercise and its derived APJ signaling and AMPK in improving the duodenal epithelial homeostasis of small intestine.

Materials and Methods

Ethical Approval.

Animal studies conducted were approved by the Institute of Animal Care and Use Committees (IACUC) at the Washington State University (ASAF# 6704) and performed in AAALAC-approved facilities in accordance with the Animals in Research: Reporting *In Vitro* Experiments (ARRIVE) guidelines (Kilkenny et al., 2012).

Animals.

To generate intestinal epithelium-specific *Apj* deleted mice, $Apj^{loxP/loxP}$ mice (Hwangbo et al., 2017; Son et al., 2020a; Son et al., 2022) were cross bred with *Vil1*-Cre-ER^{T2} (#020282, Jackson Lab) transgenic mice. Eight-week-old *Apj* deficient male mice (***Apj*^cKD**; $Apj^{loxP/loxP}$: *Vil1*-Cre-ER^{T2} (+/−)) or $Apj^{loxP/loxP}$ mice (wildtype; **WT**) were subjected to either treadmill exercise or sedentary environment: four groups 1) WT; 2) WT with exercise

(WT+Ex); 3) *Apj*^{cKD}; and 4) *Apj*^{cKD}+Ex (Fig. 1B). Before a week of exercise intervention, all mice were acclimated to treadmill exercise 3 times per week as an adaptation. Following first dose of tamoxifen injection (75 μg/g body weight) (Son et al., 2022), mice were subjected to treadmill exercise every morning. Briefly, at 48 h after tamoxifen injection, mice of exercise groups (WT+Ex and *Apj*^{cKD}+Ex) performed treadmill exercise every morning for 1 h for 3 weeks. Each training session included warming up (5 m/min for 10 min), main exercise (15 m/min for 40 min) and cooling down (5 m/min for 10 min); mice without exercise training were placed on treadmill for 1 h with speed at 0 m/min (Fig. 1). Tamoxifen was treated every week considering its half-life (Morello et al., 2003; Sanchez-Spitman et al., 2019). Mice were not exercised during the day receiving tamoxifen and the following day because of stress effects of tamoxifen (Whitfield et al., 2015). After 48 h from the last bout of exercise intervention, mice were anesthetized after 5 h fasting. Duodenum and gastrocnemius muscle were collected and stored for histological/biochemical analyses (Fig. 1A).

In addition, *Prkaa1* (AMPKα1) floxed mice (*Prkaa1*$^{loxP/loxP}$, #014141, Jackson Lab) were cross bred with *Gt(ROSA)26Sor*$^{tm1(cre/ERT)Nat}$/J mice (R26CreER, #004847, Jackson Lab) to obtain whole body inducible AMPKα1 knockdown (*Prkaa1*$^{loxP/loxP}$/ROSA^{CreER}) mice. After 48 h from the intraperitoneal (i.p.) tamoxifen injection (75 μg/g body weight) (Son et al., 2022), mice were anesthetized, and duodenum was collected and stored for biochemical analyses.

Serum biochemical analysis.

Blood was collected through heart puncture for biochemical analysis after 5 h fasting, based on our previous study (Chae et al., 2022). Serum apelin concentrations was measured using an apelin-12 enzyme immunoassay (EIA) kit (Phoenix Pharmaceuticals, Belmont, CA) (Son et al., 2020b).

Gene expression.

Total RNA (500 ng) was extracted by TRIzol reagent (Invitrogen, Grand Island, NY) and utilized for synthesizing cDNA with an iScript™ cDNA Synthesis Kit (Bio-Rad, Hercules, CA) (Chae et al., 2022). RT-qPCR was performed with SsoAdvanced™ Universal SYBR® Green Supermix (Bio-Rad) or PowerUp SYBR Green Master Mix (Applied Biosystems). 18S rRNA and/or β-actin were used for normalization. The mRNA expression was calculated via the $2^{-\Delta\Delta Ct}$ method as previously described (Chae et al., 2022). The primer sequences utilized for RT-qPCR analysis were listed in Table 1.

Quantification of mtDNA copy number.

Total DNA was extracted and utilized for measuring mitochondrial DNA (mtDNA) copy number. Briefly, mitochondrial gene, NADH dehydrogenase subunit 1 (mt*Nd1*) was normalized by genomic gene, lipoprotein lipase (*Lpl*) and analyzed based on a PCR method (Son et al., 2020a). The primer sequences were listed in Table 1.

Chromatin immunoprecipitation qPCR assay.

Chromatin immunoprecipitation (ChIP)-qPCR was performed as previously described (Yang et al., 2016b). 50 mg duodenal tissue was homogenized and cross-linked with 1% formaldehyde for 10 min and resuspended in PBS with 125 mmol/L glycine. Then, the sample was lysed in a cold ChIP lysis buffer (10 mmol/L Tris-HCl pH = 8.0, 10 mmol/L NaCl, 1% SDS, 3 mmol/L $MgCl_2$, 0.5% NP-40) with Roche complete protease inhibitor cocktail (Millipore Sigma, Burlington, MA). To extract and break up DNA into 500-800 bp fragments, lysates were sonicated and centrifuged. The supernatant was precleaned with ChIP-grade Pierce™ magnetic protein A/G beads (Thermo Scientific, Waltham, MA) and incubated with H3K4me3 (#9751; RRID: AB_2616028, Cell Signaling Technology, Danvers, MA, USA), H3K27me3 (#9733; RRID: AB_2616029, Cell Signaling Technology), or rabbit IgG antibody (30000-0-AP; RRID: AB_2819035, Proteintech, Rosemont, IL, USA). Precipitated samples with magnetic beads were treated with RNaseA and proteinase K (#25530; Thermo Fisher Scientific). Finally, obtained samples were used for ChIP-qPCR using PowerUp SYBR Green Master Mix (Applied Biosystems). The primers are listed in Table 1. Relative enrichment folds were normalized to IgG and calculated using the $2^{-\Delta\Delta Ct}$ method.

Immunoblotting.

Proteins were extracted from collected duodenum using lysis buffer (100 mM Tris-HCl, pH 6.8, 2.0% SDS, 20% glycerol, 0.02% bromophenol blue, 5% 2-mercaptoethanol, 100 mM NaF and 1 mM Na_3VO_4) and used for electrophoresis and blotting as previously described (Chae et al., 2022). Primary antibodies are listed as follows: Phospho-AMPKα (#2535; RRID: AB_331250), AMPKα (#2793; RRID: AB_915794), E-cadherin (#3195; RRID: AB_2291471), VDAC (#4661; RRID: AB_10557420) were purchased from Cell Signaling Technology (Danvers, MA, USA). APJ (#20341-1-AP; RRID: AB_2878676), PGC-1α (#66369-1-IG; RRID: AB_2828002), β-actin (#66009-1-IG), β-tubulin (#66240-1-IG), and GAPDH (#10494-1-AP) were obtained from Proteintech. Lysozyme (LYZ; #NBP2-89115; RRID: N/A) and MUC2 (#NBP1-31231; RRID: AB_10003763) were purchased from Novus Biologicals (Centennial, CO, USA). PRDM16 (#PA5-20872; RRID: AB_11154178) was purchased from Thermo Fisher Scientific (Rockford, IL, USA). β-tubulin (#E7; RRID: AB_2315513) was obtained from Developmental Studies Hybridoma Bank (Iowa City, IA, USA). As secondary antibodies, IRDye800CW (RRID: AB_621843) and IRDye680 (RRID: AB_621840) were utilized (LI-COR Biosciences, Lincoln, NE, USA). Additionally, StarBright Blue520 goat anti-rabbit IgG (#12005869) and StarBright Blue700 goat anti-mouse IgG (#12004158) were used as secondary antibodies (Bio-Rad). Blotting bands were detected using an Odyssey Infrared Imaging System (LI-COR Biosciences) or ChemiDoc™ MP Imaging System (Bio-Rad) as previously described (Chae et al., 2022; Son et al., 2022).

Histological analysis.

Collected duodenum tissues were fixed in 4% paraformaldehyde (PFA) for 24 h at room temperature and embedded in paraffin blocks. Five-μm-thick sections were utilized for hematoxylin and eosin (H&E) staining using duodenum samples as previously described (Tian et al., 2021). Besides, other sections (5-μm-thick) from duodenum

were used for immunocytochemistry (ICC) in APJ (dilution 1:50; #20341-1-AP; RRID: AB_2878676; Proteintech), MUC2 (dilution 1:50; #NBP1-31231; RRID: AB_10003763; Novus Biologicals), and LGR5 (dilution 1:50; #MA5-25644; RRID: AB_2723318; Thermo Fisher Scientific). For secondary antibodies, Alexa Fluor 555-conjugated goat anti-mouse IgG1 (dilution 1:250; #A-21127; RRID: AB_2535769; Thermo Fisher Scientific) and Alexa Fluor 555-conjugated donkey anti-rabbit IgG (dilution 1:250; #406412; RRID: AB_2563181; BioLegend, San Diego, CA, USA) were used. The villus and crypt lengths and the number of the positive cells were measured in ImageJ (NIH) according to a previous report (Son et al., 2020a).

Statistical analysis.

Statistical analyses were conducted using SPSS Statistics ver.21 (IBM Corp., Armonk, NY, USA). Results were reported as mean ± SD, and statistical significance was defined as $P < 0.05$, which was indicated by Student *t* test or two-way ANOVA with Tukey's test. Pearson correlations were used to compare the relationship between variables. Statistical differences were determined as * or $^{\#}P < 0.05$, ** or $^{\#\#}P < 0.01$, and ***, ### or $^{\$\$\$}P < 0.001$.

Results

Exercise improves small intestinal epithelium by activating APJ signaling.

Previous studies have elucidated that apelin reduces adiposity and improves glucose and insulin metabolism in adipose tissue and skeletal muscle via activation of APJ signaling (Higuchi et al., 2007; Castan-Laurell et al., 2012; Hu et al., 2016). However, the role of APJ in intestinal epithelium remains to be defined. To examine, we deleted *Apj* specifically in intestinal epithelium using a tamoxifen inducible Cre ($Apj^{loxP/loxP}$:$Vil1^{CreER}$) (Fig. 2A). Following tamoxifen injection, deletion of *Apj* in the intestinal epithelium reduced APJ levels in the small intestine (Fig. 2B). Because epithelial cells only account for a portion of intestinal cells, we further confirmed that the absence of APJ protein in gut epithelium by immunohistochemical staining (Fig. 2C). *Apj* deletion reduced body weight, whereas exercise decreased the body weight of wild-type (WT) floxed mice, not in APJ knockout (KO) mice (Fig. 2D). H&E staining showed that the small intestine of *Apj* KO mice contained disorganized columnar epithelium and underwent progressive crypt shortening (Fig. 2E). On the other hand, exercise made the length of villi and crypts of small intestine longer (Fig. 2E). Consistent with benefits of exercise, the lengthening villi and crypts were negatively associated with their body weights, but these differences were absent in *Apj* KO mice (Fig. 2F). Together, these data showed that exercise enhances the formation of villus and crypt epithelium via APJ activation.

Exercise enhances villus remodeling through activating APJ signaling.

Because both villus and crypt lengths were increased in response to exercise (Fig. 2E), we assessed villus morphological changes (Fig. 3A). The number of villus epithelial cells were increased in response to exercise in the WT intestine (Fig. 3B), which was abolished due to *Apj* KD (Fig. 3B). The *Apj* ablation decreased the expression of MUC2, a marker for goblet cells (Fig. 3C). Consistently, exercise increased the expression of *Muc2* and its protein contents in the WT intestine (Fig. 3D, E); such effect was absent due to *Apj* deletion

(Fig. 3D, E). The *Apj* KO also decreased the expression of marker genes of secretary cells, including *Mmp7* (Paneth cells), *Tff3* (Goblet cells), and *Reg4* (Enteroendocrine cells) (Fig. 3D). Exercise increased the expression of these secretory marker genes in the WT, but not in *Apj* deleted small intestine (Fig. 3D). However, exercise or *Apj* deletion did not change the expression of tuft cell marker, *Dclk1* (Fig. 3D). The expression of differentiated epithelial marker, E-cadherin, was increased in response to exercise, but not in *Apj* deleted mice (Fig. 3E). Taken together, we showed that exercise-mediated APJ signaling facilitates villus remodeling.

Apj is required for enhanced crypt remodeling of the small intestine in response to exercise.

Crypt progenitor cells proliferate and migrate up the villi to generate differentiated intestinal epithelium (Kwon et al., 2020). We further analyzed crypt cell markers. The number of epithelial cells of a crypt were increased in response to exercise in the WT intestine only, not in *Apj* deleted intestine (Fig. 4A). LGR5+ intestinal crypt stem cells build crypt-villus structures (Sato et al., 2009). Immunocytochemical staining of the small intestine showed that LGR5+ cells were reduced in *Apj* deleted crypts (Fig. 4B). Consistently, the number of LGR5+ cells was increased in the WT crypts in response to exercise, not in *Apj* deleted mice (Fig. 4C). Expression of *Lgr5* and crypt marker genes, including *Lyz1*, *Olfm4* (stem cell marker), and *Bmi1* was impeded by deletion of *Apj* (Fig. 4D, E). Consistently, as a crypt marker, LYZ protein expression was reduced in *Apj* deficient intestine (Fig. 4F). Together, these data demonstrate that APJ signaling stimulated by exercise promotes the structural remodeling of villi and crypts in the small intestine.

Exercise-induced APJ signaling enhances mitochondrial biogenesis and fatty acid metabolism in the small intestine.

Mitochondrial biogenesis is essential for epithelial differentiation (Urbauer et al., 2020). Thus, we analyzed mitochondrial biogenic markers. Exercise increased mitochondrial DNA (mtDNA) copy number in WT but not in APJ KO intestine (Fig. 5C). Furthermore, APJ was required for the elevated expression of mitochondrial biogenic genes, including *Ppargc1a* (a transcriptional coactivator inducing mitochondrial biogenesis) and *Tfam* (a mitochondrial transcription factor A), in response to exercise (Fig. 5D). Additionally, exercise increased mitochondrial outer membrane activity related marker, VDAC, and biogenic marker, PGC-1α of both full length (FL) and truncated N-terminal (NT) isoforms, dependent on the presence of APJ (Fig. 5F). These data demonstrate that exercise enhances mitochondrial biogenesis in small intestine which is dependent on APJ signaling.

Mitochondria are responsible for oxidative metabolism, and PRDM16 enhances intestinal epithelial oxidative metabolism including FAO (Stine et al., 2019b). Consistently, exercise dramatically upregulated the expression of *Prdm16* gene and protein content via APJ activation (Fig. 5A, B). *Cpt1a* encodes an enzyme in the mitochondrial outer membrane, which converts acyl-CoA species to acyl-carnitines (Lee et al., 2011) and CPT2 is in the mitochondrial inner membrane, both of which are critical for fatty acid importation into mitochondria for oxidation. Exercise increased *Cpt1a* and *Cpt2* expression (Fig. 5D). Moreover, exercise also increased the expression of other genes, involved in FAO, including

Acadm, *Acaa2*, and *Hadh* and mitochondrial respiration markers, which were dependent on the presence of APJ (Fig. 5D). Consistent with the exercise-induced PRDM16/CPT1A/FAO activation, PRDM16 was positively associated with mitochondria input and the expression of FAO genes (Fig. 5G). Taken together, our data show that exercise induces the expression of *Prdm16* and mitochondrial fatty acid oxidative genes.

Exercise stimulates AMPK activation regulating duodenal epithelial homeostasis.

Exercise promotes mitochondrial biogenesis and FAO, which is dependent on APJ signaling (Fig. 5). AMP-activated protein kinase (AMPK) locates down-stream of APJ signaling and AMPK is highly expressed in intestinal epithelium (Sun et al., 2017). Consistently, exercise dramatically upregulated AMPK phosphorylation in WT, but not in *Apj* deleted intestine (Fig. 6A). To test the role of AMPK, we deleted AMPKα1 and investigated intestinal epithelial remodeling in the duodenum (Fig. 6B,C). Of note, we found that epithelial cell markers of MUC2 and E-cadherin were dramatically downregulated in the AMPK deficient duodenum (Fig. 6D). Furthermore, PRDM16, responsible for mitochondrial oxidative metabolism and mitochondrial biogenic markers were downregulated in the AMPK deficiency (Fig. 6E,F). These data are consistent with the increase in epithelial cell numbers of both crypts and villi (Fig. 3B and 4A). Taken together, these data show that exercise not only enhances AMPK phosphorylation, but also AMPK-dependent duodenal epithelial remodeling, thereby enhancing intestinal formation and function (Fig. 6G).

Exercise induces exerkine apelin secretion from skeletal muscle.

Apelin is recognized as an exerkine secreted from skeletal muscle in response to exercise training (Besse-Patin et al., 2014; Son et al., 2017). Secreted apelin into the circulation has an endocrinological role in other organs (Besse-Patin et al., 2014; Fournel et al., 2017). Similar to the previous studies (Besse-Patin et al., 2014; Fournel et al., 2017), we found that apelin gene expression was dominantly expressed in skeletal muscle than other tissues, including liver, inguinal white adipose tissue (ingWAT), and duodenum small intestine, and apelin was more upregulated in response to exercise training (Fig. 7C). Since we utilized intestine-specific APJ deficient mice, the skeletal muscle has normal expression of apelin (Apj^{cKD} × Exercise) (Fig. 7B). We also found that exercise training increased expression of apelin in muscle and the circulating apelin level regardless of intestinal APJ deficiency, suggesting that skeletal muscle is a major origin of circulating apelin secreted in response to exercise (Fig. 7A–D). Together, we found that skeletal muscle secretes apelin into the circulation, which might be the major origin of apelin in improving intestinal epithelial homeostasis (Fig. 7E).

APJ-AMPK mediates exercise-induced duodenal histone modifications.

We previously reported that exercise-induced apelin signaling dynamically regulated epigenetic modifications of *Prdm16* promoter via AMPK, α-ketoglutarate (α-KG), and ten-eleven translocations (TETs) (Yang et al., 2016b; Son et al., 2020b). In addition, histone modifications occur in response to exercise adaptations (McGee & Hargreaves, 2011). Therefore, based on our previous studies showing the presence of CpG islands in the *Prdm16* promoter (Yang et al., 2016b; Son et al., 2020b), we analyzed enrichment folds of histone H3 lysine 27 tri-methylation (H3K27me3) and histone H3 lysine 4 tri-methylation

(H3K4me3) in the intestine-specific APJ deficient or AMPK deficient duodenum (Fig. 8A). H3K27me3 (gene silencing) was decreased in response to exercise training only in the intestine of wild-type mice, but not in intestine-specific APJ deletion (Fig. 8B). On the other hand, H3K4me3 (gene activation) was elevated due to exercise, but not after APJ deletion (Fig. 8B). In AMPK deleted duodenum, H3K27me3 was increased, but H3K4me3 was decreased (Fig. 8C). Consistently, TET family was upregulated by exercise, but they were downregulated by APJ or AMPK deletion in the duodenum (Fig. 8D,E). On the other hand, no changes in IDH family were discovered in APJ deficient mice with/without exercise or AMPK deletion (Fig. 8D,E). Together, these showed that exercise-dependent PRDM16 expression is regulated by alteration of APJ-AMPK-mediated histone modifications (Fig. 8F).

Discussion

In our previous studies, we showed that apelin-APJ signaling is exercise-dependently regulated (Son et al., 2020a; Son et al., 2022). The current study showed that exercise enhances epithelial structure and homeostasis, especially in both villus and crypt, which is mediated by APJ activation. Of note, the improvement of intestinal epithelium was associated with enhanced mitochondrial biogenesis and activation of mitochondrial oxidative metabolism, which accelerates intestinal epithelial remodeling. As a potential underlying signaling pathway, we also showed that exercise enhances AMPK phosphorylation, which is dependently regulated by APJ activation. Consistently, duodenal epithelial remodeling and expression of PRDM16 enhancing mitochondrial oxidative metabolism were mediated by AMPK activation. Moreover, PRDM16 was epigenetically upregulated by histone modifications, improving duodenal epithelial structure and homeostasis.

The functional maintenance of intestinal epithelium is critically important for the digestion of food and absorption of nutrients (Kong et al., 2018), which are regulated by intestinal epithelial homeostasis, including differentiation, proliferation, and renewal (Kong et al., 2018). The TA cells produced by ISCs in the crypts migrate to the villus while differentiating into the villus epithelial cells (Snippert et al., 2010; Kurokawa et al., 2020). And, this renewal and migration process occur continuously with the whole epithelium replaced in every 4 to 5 days (Clevers, 2013). Given that chronic exercise improves gut integrity (Keirns et al., 2020), we hypothesized that exercise improves intestinal renewal and migration. The present study underscores an important signaling axis, exercise-induced APJ-AMPK axis, in regulating the homeostasis of intestinal epithelium. The epithelial integrity is critically important for health, with its disruption leading to inflammatory bowel diseases, autoimmune diseases and metabolic dysfunctions (Urbauer et al., 2020; Gieryńska et al., 2022). In addition, gut epithelial disruption affects gut microbial composition, which in turn affects host health (Monda et al., 2017). Gut microbiota is closely associated with maintaining epithelial barrier functions and gut homeostasis (Eckburg et al., 2005; O'Hara & Shanahan, 2006).

APJ, a G protein-coupled receptor, has been traditionally recognized as a mediator in regulating metabolism and combating against obesity-induced metabolic dysfunction (Hu

et al., 2021; Li et al., 2022). Furthermore, it involves in the regulation of digestion and pathologic responses of the gastrointestinal tract (Huang et al., 2019). Consistently, we found that APJ deletion reduced body weight, which might be due to impaired epithelial function and its-derived decrease in absorptive function (Kraehenbuhl et al., 1997). Mechanistically, APJ signaling may generate beneficial effects through two complementary pathways: 1) APJ-dependent $G\alpha_q$ in activating AMPK signaling (Yue et al., 2011), which stimulates mitochondrial biogenesis (Herzig & Shaw, 2018) and browning adipogenesis (Daval et al., 2006; Desjardins & Steinberg, 2018); and 2) APJ-dependent $G\alpha_i$ activation(Nakano et al., 2017) in promoting lipolysis (Choi et al., 2010; Huang et al., 2018) and cell proliferation (Yu & Cui, 2016). Fundamentally, exercise is a dynamic regulator of AMPK signaling (Jørgensen et al., 2006; Niederberger et al., 2015; Spaulding & Yan, 2022), which further stimulates PGC-1α (Ferraro et al., 2014), a pivotal co-activator of mitochondrial energy metabolism (Liang & Ward, 2006) (Lira et al., 2010). Consistently, AMPK improves intestinal epithelial differentiation and barrier function (Sun et al., 2017). Thus, we propose an exercise-APJ-AMPK-PGC-1α axis, which improves the intestinal epithelium via accelerating mitochondrial biogenesis and oxidative metabolism (Yang et al., 2016a).

In addition to AMPK-PGC-1α-induced energy metabolism, it has recently discovered that PRDM16 enhances small intestinal epithelial renewal through enhancing FAO, and the oxidative level in duodenum is especially high (Stine et al., 2019a). It stimulates the expression of CD36 and the concentration of acyl-CoA to enhance fatty acid uptake in the intestine (Zhao et al., 2021). CPT1A is a rate-limiting enzyme of FAO, which catalyzes the conversion of acyl-CoA into acyl-carnitine to enter mitochondria (Schlaepfer & Joshi, 2020). Also, ACADM and ACAA2 are essential for β-oxidation of fatty acids (Zhang et al., 2018; Ibrahim & Temtem, 2022). Consistently, the expression of CPT1A, ACADM, and ACAA2 was regulated by PRDM16 activation in intestinal duodenum (Stine et al., 2019a).

Although histone modifications occur in response to exercise adaptations (McGee & Hargreaves, 2011), apelin signaling and AMPK-mediated histone modifications in developing intestinal epithelium have not been addressed. Previously, the evidence has been reported, emphasizing that physical activity regulates skeletal muscle development by histone modifications (McGee et al., 2009). In particular, histone modifications of H3K27me3 and H3K4me3 in pre-implantation embryos are closely associated with gene repression (H3K27me3) and activation (H3K4me3) (Liu et al., 2016). We previously showed a great abundance of H3K27me3 and H3K4me3 existed in the *Prdm16* promoter (Yang et al., 2016b). TETs mediate DNA demethylation (Wu & Zhang, 2017), whereas the mutation of IDH, a key enzyme converting isocitrate to α-KG, blocks histone demethylation (Lu et al., 2012).

In summary, we have demonstrated that treadmill exercise enhances the structure and remodeling of villus and crypt in the duodenum via APJ signaling activation. Exercise-induced APJ-AMPK axis not only promotes mitochondrial biogenesis, but also activates PRDM16-induced oxidative metabolism, improving the structure of villus-crypt epithelium. Of note, exercise induces histone modifications to activate PRDM16 expression via APJ-

AMPK axis. Our finding implicates the clinical importance and applications of exercise training and respective signaling pathways in enhancing intestinal epithelial homeostasis.

Supplementary Material

Refer to Web version on PubMed Central for supplementary material.

Acknowledgements.

We thank the laboratory members of Drs. Son, Du, and Zhu for their technical assistance.

Funding.

This work was supported by the National Institutes of Health Grant R01-HD067449 to M.D. and USDA-NIFA grant 2018-67017-27517 to M-J.Z.

First Author Biography

Dr. Songah Chae received her Ph.D. (2022) in the Department of Animal Sciences at Washington State University, Pullman, Washington. Currently, Dr. Chae is a Postdoctoral Fellow at University of Maryland School of Medicine, Baltimore, Maryland. Her research interest is maternal exercise and its effects on fetal development, focusing on intestinal and placental development. Her work ultimately aims to the translation into clinical practice to improve health outcomes for mothers and children affected by obesity.

Data availability statement.

The data that support the findings of this study are available from the corresponding author upon reasonable request.

References

Ando W, Yokomori H, Otori K & Oda M. (2017). The Apelin Receptor APJ in Hematopoietic Stem Cells/Progenitor Cells in the Early Stage of Non-Alcoholic Steatohepatitis. Journal of clinical medicine research 9, 809–811. [PubMed: 28811860]

Bertrand C, Valet P & Castan-Laurell I. (2015). Apelin and energy metabolism. Frontiers in physiology 6, 115. [PubMed: 25914650]

Besse-Patin A, Montastier E, Vinel C, Castan-Laurell I, Louche K, Dray C, Daviaud D, Mir L, Marques MA, Thalamas C, Valet P, Langin D, Moro C & Viguerie N. (2014). Effect of endurance training on skeletal muscle myokine expression in obese men: identification of apelin as a novel myokine. International journal of obesity (2005) 38, 707–713. [PubMed: 23979219]

Beyaz S, Mana MD, Roper J, Kedrin D, Saadatpour A, Hong SJ, Bauer-Rowe KE, Xifaras ME, Akkad A, Arias E, Pinello L, Katz Y, Shinagare S, Abu-Remaileh M, Mihaylova MM, Lamming DW, Dogum R, Guo G, Bell GW, Selig M, Nielsen GP, Gupta N, Ferrone CR, Deshpande V, Yuan GC, Orkin SH, Sabatini DM & Yilmaz ÖH. (2016). High-fat diet enhances stemness and tumorigenicity of intestinal progenitors. Nature 531, 53–58. [PubMed: 26935695]

Blanpain C, Horsley V & Fuchs E. (2007). Epithelial stem cells: turning over new leaves. Cell 128, 445–458. [PubMed: 17289566]

Castan-Laurell I, Dray C, Knauf C, Kunduzova O & Valet P. (2012). Apelin, a promising target for type 2 diabetes treatment? Trends in endocrinology and metabolism: TEM 23, 234–241. [PubMed: 22445464]

Chae SA, Son JS, Zhao L, Gao Y, Liu X, Marie de Avila J, Zhu MJ & Du M. (2022). Exerkine apelin reverses obesity-associated placental dysfunction by accelerating mitochondrial biogenesis in mice. American journal of physiology Endocrinology and metabolism 322, E467–e479. [PubMed: 35403440]

Choi SM, Tucker DF, Gross DN, Easton RM, DiPilato LM, Dean AS, Monks BR & Birnbaum MJ. (2010). Insulin regulates adipocyte lipolysis via an Akt-independent signaling pathway. Molecular and cellular biology 30, 5009–5020. [PubMed: 20733001]

Clevers H (2013). The intestinal crypt, a prototype stem cell compartment. Cell 154, 274–284. [PubMed: 23870119]

Daval M, Foufelle F & Ferré P. (2006). Functions of AMP-activated protein kinase in adipose tissue. The Journal of physiology 574, 55–62. [PubMed: 16709632]

Desjardins EM & Steinberg GR. (2018). Emerging Role of AMPK in Brown and Beige Adipose Tissue (BAT): Implications for Obesity, Insulin Resistance, and Type 2 Diabetes. Current diabetes reports 18, 80. [PubMed: 30120579]

Eckburg PB, Bik EM, Bernstein CN, Purdom E, Dethlefsen L, Sargent M, Gill SR, Nelson KE & Relman DA. (2005). Diversity of the human intestinal microbial flora. Science (New York, NY) 308, 1635–1638.

Ferraro E, Giammarioli AM, Chiandotto S, Spoletini I & Rosano G. (2014). Exercise-induced skeletal muscle remodeling and metabolic adaptation: redox signaling and role of autophagy. Antioxidants & redox signaling 21, 154–176. [PubMed: 24450966]

Folmes CD, Dzeja PP, Nelson TJ & Terzic A. (2012). Metabolic plasticity in stem cell homeostasis and differentiation. Cell stem cell 11, 596–606. [PubMed: 23122287]

Fournel A, Drougard A, Duparc T, Marlin A, Brierley SM, Castro J, Le-Gonidec S, Masri B, Colom A, Lucas A, Rousset P, Cenac N, Vergnolle N, Valet P, Cani PD & Knauf C. (2017). Apelin targets gut contraction to control glucose metabolism via the brain. Gut 66, 258–269. [PubMed: 26565000]

Gieryńska M, Szulc-Dąbrowska L, Struzik J, Mielcarska MB & Gregorczyk-Zboroch KP. (2022). Integrity of the Intestinal Barrier: The Involvement of Epithelial Cells and Microbiota-A Mutual Relationship. Animals : an open access journal from MDPI 12.

Herzig S & Shaw RJ. (2018). AMPK: guardian of metabolism and mitochondrial homeostasis. Nature reviews Molecular cell biology 19, 121–135. [PubMed: 28974774]

Higuchi K, Masaki T, Gotoh K, Chiba S, Katsuragi I, Tanaka K, Kakuma T & Yoshimatsu H. (2007). Apelin, an APJ receptor ligand, regulates body adiposity and favors the messenger ribonucleic acid expression of uncoupling proteins in mice. Endocrinology 148, 2690–2697. [PubMed: 17347313]

Hou J, Wang L, Long H, Wu H, Wu Q, Zhong T, Chen X, Zhou C, Guo T & Wang T. (2017). Hypoxia preconditioning promotes cardiac stem cell survival and cardiogenic differentiation in vitro involving activation of the HIF-1α/apelin/APJ axis. Stem cell research & therapy 8, 215. [PubMed: 28962638]

Hu G, Wang Z, Zhang R, Sun W & Chen X. (2021). The Role of Apelin/Apelin Receptor in Energy Metabolism and Water Homeostasis: A Comprehensive Narrative Review. Frontiers in physiology 12, 632886. [PubMed: 33679444]

Hu H, He L, Li L & Chen L. (2016). Apelin/APJ system as a therapeutic target in diabetes and its complications. Molecular genetics and metabolism 119, 20–27. [PubMed: 27650065]

Huang X, Liu G, Guo J & Su Z. (2018). The PI3K/AKT pathway in obesity and type 2 diabetes. International journal of biological sciences 14, 1483–1496. [PubMed: 30263000]

Huang Z, Luo X, Liu M & Chen L. (2019). Function and regulation of apelin/APJ system in digestive physiology and pathology. Journal of cellular physiology 234, 7796–7810. [PubMed: 30390294]

Hwangbo C, Wu J, Papangeli I, Adachi T, Sharma B, Park S, Zhao L, Ju H, Go GW, Cui G, Inayathullah M, Job JK, Rajadas J, Kwei SL, Li MO, Morrison AR, Quertermous T, Mani A,

Red-Horse K & Chun HJ. (2017). Endothelial APLNR regulates tissue fatty acid uptake and is essential for apelin's glucose-lowering effects. Science translational medicine 9.

Ibrahim S & Temtem T. (2022). Medium-Chain Acyl-COA Dehydrogenase Deficiency. In StatPearls. StatPearls Publishing Copyright © 2022, StatPearls Publishing LLC., Treasure Island (FL).

Ji W, Gong L, Wang J, He H & Zhang Y. (2017). Hypoxic Exercise Training Promotes apelin/APJ Expression in Skeletal Muscles of High Fat Diet-Induced Obese Mice. Protein and peptide letters 24, 64–70. [PubMed: 27834140]

Jørgensen SB, Richter EA & Wojtaszewski JF. (2006). Role of AMPK in skeletal muscle metabolic regulation and adaptation in relation to exercise. The Journal of physiology 574, 17–31. [PubMed: 16690705]

Keirns BH, Koemel NA, Sciarrillo CM, Anderson KL & Emerson SR. (2020). Exercise and intestinal permeability: another form of exercise-induced hormesis? American journal of physiology Gastrointestinal and liver physiology 319, G512–g518. [PubMed: 32845171]

Kilkenny C, Browne WJ, Cuthill IC, Emerson M & Altman DG. (2012). Improving bioscience research reporting: the ARRIVE guidelines for reporting animal research. Osteoarthritis and cartilage 20, 256–260. [PubMed: 22424462]

Kong S, Zhang YH & Zhang W. (2018). Regulation of Intestinal Epithelial Cells Properties and Functions by Amino Acids. BioMed research international 2018, 2819154. [PubMed: 29854738]

Kraehenbuhl JP, Pringault E & Neutra MR. (1997). Review article: Intestinal epithelia and barrier functions. Alimentary pharmacology & therapeutics 11 Suppl 3, 3–8; discussion 8-9.

Kurokawa K, Hayakawa Y & Koike K. (2020). Plasticity of Intestinal Epithelium: Stem Cell Niches and Regulatory Signals. International journal of molecular sciences 22. [PubMed: 33375004]

Kwon O, Han TS & Son MY. (2020). Intestinal Morphogenesis in Development, Regeneration, and Disease: The Potential Utility of Intestinal Organoids for Studying Compartmentalization of the Crypt-Villus Structure. Front Cell Dev Biol 8, 593969. [PubMed: 33195268]

Lee K, Kerner J & Hoppel CL. (2011). Mitochondrial carnitine palmitoyltransferase 1a (CPT1a) is part of an outer membrane fatty acid transfer complex. J Biol Chem 286, 25655–25662. [PubMed: 21622568]

Li C, Cheng H, Adhikari BK, Wang S, Yang N, Liu W, Sun J & Wang Y. (2022). The Role of Apelin-APJ System in Diabetes and Obesity. Front Endocrinol (Lausanne) 13, 820002. [PubMed: 35355561]

Li LC & Dahiya R. (2002). MethPrimer: designing primers for methylation PCRs. Bioinformatics (Oxford, England) 18, 1427–1431. [PubMed: 12424112]

Liang H & Ward WF. (2006). PGC-1alpha: a key regulator of energy metabolism. Advances in physiology education 30, 145–151. [PubMed: 17108241]

Lin HT, Otsu M & Nakauchi H. (2013). Stem cell therapy: an exercise in patience and prudence. Philosophical transactions of the Royal Society of London Series B, Biological sciences 368, 20110334. [PubMed: 23166396]

Lira VA, Benton CR, Yan Z & Bonen A. (2010). PGC-1alpha regulation by exercise training and its influences on muscle function and insulin sensitivity. American journal of physiology Endocrinology and metabolism 299, E145–161. [PubMed: 20371735]

Liu X, Wang C, Liu W, Li J, Li C, Kou X, Chen J, Zhao Y, Gao H, Wang H, Zhang Y, Gao Y & Gao S. (2016). Distinct features of H3K4me3 and H3K27me3 chromatin domains in pre-implantation embryos. Nature 537, 558–562. [PubMed: 27626379]

Lu C, Ward PS, Kapoor GS, Rohle D, Turcan S, Abdel-Wahab O, Edwards CR, Khanin R, Figueroa ME, Melnick A, Wellen KE, O'Rourke DM, Berger SL, Chan TA, Levine RL, Mellinghoff IK & Thompson CB. (2012). IDH mutation impairs histone demethylation and results in a block to cell differentiation. Nature 483, 474–478. [PubMed: 22343901]

McGee SL, Fairlie E, Garnham AP & Hargreaves M. (2009). Exercise-induced histone modifications in human skeletal muscle. The Journal of physiology 587, 5951–5958. [PubMed: 19884317]

McGee SL & Hargreaves M. (2011). Histone modifications and exercise adaptations. Journal of applied physiology (Bethesda, Md : 1985) 110, 258–263. [PubMed: 21030677]

Mihaylova MM, Cheng CW, Cao AQ, Tripathi S, Mana MD, Bauer-Rowe KE, Abu-Remaileh M, Clavain L, Erdemir A, Lewis CA, Freinkman E, Dickey AS, La Spada AR, Huang Y, Bell GW,

Deshpande V, Carmeliet P, Katajisto P, Sabatini DM & Yilmaz ÖH. (2018). Fasting Activates Fatty Acid Oxidation to Enhance Intestinal Stem Cell Function during Homeostasis and Aging. Cell stem cell 22, 769–778.e764. [PubMed: 29727683]

Monda V, Villano I, Messina A, Valenzano A, Esposito T, Moscatelli F, Viggiano A, Cibelli G, Chieffi S, Monda M & Messina G. (2017). Exercise Modifies the Gut Microbiota with Positive Health Effects. Oxid Med Cell Longev 2017, 3831972. [PubMed: 28357027]

Morello KC, Wurz GT & DeGregorio MW. (2003). Pharmacokinetics of selective estrogen receptor modulators. Clinical pharmacokinetics 42, 361–372. [PubMed: 12648026]

Nakano N, Matsuda S, Ichimura M, Minami A, Ogino M, Murai T & Kitagishi Y. (2017). PI3K/AKT signaling mediated by G protein-coupled receptors is involved in neurodegenerative Parkinson's disease (Review). International journal of molecular medicine 39, 253–260. [PubMed: 28000847]

Niederberger E, King TS, Russe OQ & Geisslinger G. (2015). Activation of AMPK and its Impact on Exercise Capacity. Sports medicine (Auckland, NZ) 45, 1497–1509.

O'Carroll AM, Lolait SJ, Harris LE & Pope GR. (2013). The apelin receptor APJ: journey from an orphan to a multifaceted regulator of homeostasis. The Journal of endocrinology 219, R13–35. [PubMed: 23943882]

O'Hara AM & Shanahan F. (2006). The gut flora as a forgotten organ. EMBO reports 7, 688–693. [PubMed: 16819463]

Sanchez-Spitman AB, Swen JJ, Dezentje VO, Moes D, Gelderblom H & Guchelaar HJ. (2019). Clinical pharmacokinetics and pharmacogenetics of tamoxifen and endoxifen. Expert review of clinical pharmacology 12, 523–536. [PubMed: 31008668]

Sato T, Vries RG, Snippert HJ, van de Wetering M, Barker N, Stange DE, van Es JH, Abo A, Kujala P, Peters PJ & Clevers H. (2009). Single Lgr5 stem cells build crypt-villus structures in vitro without a mesenchymal niche. Nature 459, 262–265. [PubMed: 19329995]

Schlaepfer IR & Joshi M. (2020). CPT1A-mediated Fat Oxidation, Mechanisms, and Therapeutic Potential. Endocrinology 161. [PubMed: 33213120]

Snippert HJ, van der Flier LG, Sato T, van Es JH, van den Born M, Kroon-Veenboer C, Barker N, Klein AM, van Rheenen J, Simons BD & Clevers H. (2010). Intestinal crypt homeostasis results from neutral competition between symmetrically dividing Lgr5 stem cells. Cell 143, 134–144. [PubMed: 20887898]

Son JS, Chae SA, Wang H, Chen Y, Bravo Iniguez A, de Avila JM, Jiang Z, Zhu MJ & Du M. (2020a). Maternal Inactivity Programs Skeletal Muscle Dysfunction in Offspring Mice by Attenuating Apelin Signaling and Mitochondrial Biogenesis. Cell reports 33, 108461. [PubMed: 33264618]

Son JS, Chae SA, Zhao L, Wang H, de Avila JM, Zhu MJ, Jiang Z & Du M. (2022). Maternal exercise intergenerationally drives muscle-based thermogenesis via activation of apelin-AMPK signaling. EBioMedicine 76, 103842. [PubMed: 35081489]

Son JS, Kim HJ, Son Y, Lee H, Chae SA, Seong JK & Song W. (2017). Effects of exercise-induced apelin levels on skeletal muscle and their capillarization in type 2 diabetic rats. Muscle & nerve 56, 1155–1163. [PubMed: 28164323]

Son JS, Zhao L, Chen Y, Chen K, Chae SA, de Avila JM, Wang H, Zhu MJ, Jiang Z & Du M. (2020b). Maternal exercise via exerkine apelin enhances brown adipogenesis and prevents metabolic dysfunction in offspring mice. Science advances 6, eaaz0359. [PubMed: 32494609]

Spaulding HR & Yan Z. (2022). AMPK and the Adaptation to Exercise. Annual review of physiology 84, 209–227.

Stine RR, Sakers AP, TeSlaa T, Kissig M, Stine ZE, Kwon CW, Cheng L, Lim HW, Kaestner KH, Rabinowitz JD & Seale P. (2019a). PRDM16 Maintains Homeostasis of the Intestinal Epithelium by Controlling Region-Specific Metabolism. Cell stem cell 25, 830–845.e838. [PubMed: 31564549]

Stine RR, Sakers AP, TeSlaa T, Kissig M, Stine ZE, Kwon CW, Cheng L, Lim HW, Kaestner KH, Rabinowitz JD & Seale P. (2019b). PRDM16 Maintains Homeostasis of the Intestinal Epithelium by Controlling Region-Specific Metabolism. Cell stem cell 25, 830–845 e838. [PubMed: 31564549]

Sun X, Yang Q, Rogers CJ, Du M & Zhu MJ. (2017). AMPK improves gut epithelial differentiation and barrier function via regulating Cdx2 expression. Cell death and differentiation 24, 819–831. [PubMed: 28234358]

Than A, He HL, Chua SH, Xu D, Sun L, Leow MK & Chen P. (2015). Apelin Enhances Brown Adipogenesis and Browning of White Adipocytes. J Biol Chem 290, 14679–14691. [PubMed: 25931124]

Tian Q, Bravo Iniguez A, Sun Q, Wang H, Du M & Zhu MJ. (2021). Dietary Alpha-Ketoglutarate Promotes Epithelial Metabolic Transition and Protects against DSS-Induced Colitis. Molecular nutrition & food research 65, e2000936. [PubMed: 33547710]

Urbauer E, Rath E & Haller D. (2020). Mitochondrial Metabolism in the Intestinal Stem Cell Niche-Sensing and Signaling in Health and Disease. Front Cell Dev Biol 8, 602814. [PubMed: 33469536]

Wang G, Anini Y, Wei W, Qi X, AM OC, Mochizuki T, Wang HQ, Hellmich MR, Englander EW & Greeley GH Jr. (2004). Apelin, a new enteric peptide: localization in the gastrointestinal tract, ontogeny, and stimulation of gastric cell proliferation and of cholecystokinin secretion. Endocrinology 145, 1342–1348. [PubMed: 14670994]

Whitfield J, Littlewood T & Soucek L. (2015). Tamoxifen administration to mice. Cold Spring Harbor protocols 2015, 269–271. [PubMed: 25734062]

Wu X & Zhang Y. (2017). TET-mediated active DNA demethylation: mechanism, function and beyond. Nat Rev Genet 18, 517–534. [PubMed: 28555658]

Yang H, Wang X, Xiong X & Yin Y. (2016a). Energy metabolism in intestinal epithelial cells during maturation along the crypt-villus axis. Scientific reports 6, 31917. [PubMed: 27558220]

Yang Q, Liang X, Sun X, Zhang L, Fu X, Rogers CJ, Berim A, Zhang S, Wang S, Wang B, Foretz M, Viollet B, Gang DR, Rodgers BD, Zhu MJ & Du M. (2016b). AMPK/alpha-Ketoglutarate Axis Dynamically Mediates DNA Demethylation in the Prdm16 Promoter and Brown Adipogenesis. Cell metabolism 24, 542–554. [PubMed: 27641099]

Yu JS & Cui W. (2016). Proliferation, survival and metabolism: the role of PI3K/AKT/mTOR signalling in pluripotency and cell fate determination. Development (Cambridge, England) 143, 3050–3060. [PubMed: 27578176]

Yue P, Jin H, Xu S, Aillaud M, Deng AC, Azuma J, Kundu RK, Reaven GM, Quertermous T & Tsao PS. (2011). Apelin decreases lipolysis via G(q), G(i), and AMPK-Dependent Mechanisms. Endocrinology 152, 59–68. [PubMed: 21047945]

Zhang J, Ren CX, Qi YF, Lou LX, Chen L, Zhang LK, Wang X & Tang C. (2006). Exercise training promotes expression of apelin and APJ of cardiovascular tissues in spontaneously hypertensive rats. Life sciences 79, 1153–1159. [PubMed: 16674982]

Zhang Y, Wang Y, Wang X, Ji Y, Cheng S, Wang M, Zhang C, Yu X, Zhao R, Zhang W, Jin J, Li T, Zuo Q & Li B. (2018). Acetyl-coenzyme A acyltransferase 2 promote the differentiation of sheep precursor adipocytes into adipocytes. Journal of cellular biochemistry.

Zhao L, Li Y, Ding Q, Li Y, Chen Y & Ruan XZ. (2021). CD36 Senses Dietary Lipids and Regulates Lipids Homeostasis in the Intestine. Frontiers in physiology 12, 669279. [PubMed: 33995128]

Key points

- APJ signaling is required for improved epithelial homeostasis of the small intestine in response to exercise.
- Exercise intervention activates PRDM16 through inducing histone modifications, improving mitochondrial biogenesis and fatty acid metabolism in duodenum.
- Structure of intestinal epithelium is improved by muscle-derived exerkine apelin through APJ-AMPK axis.

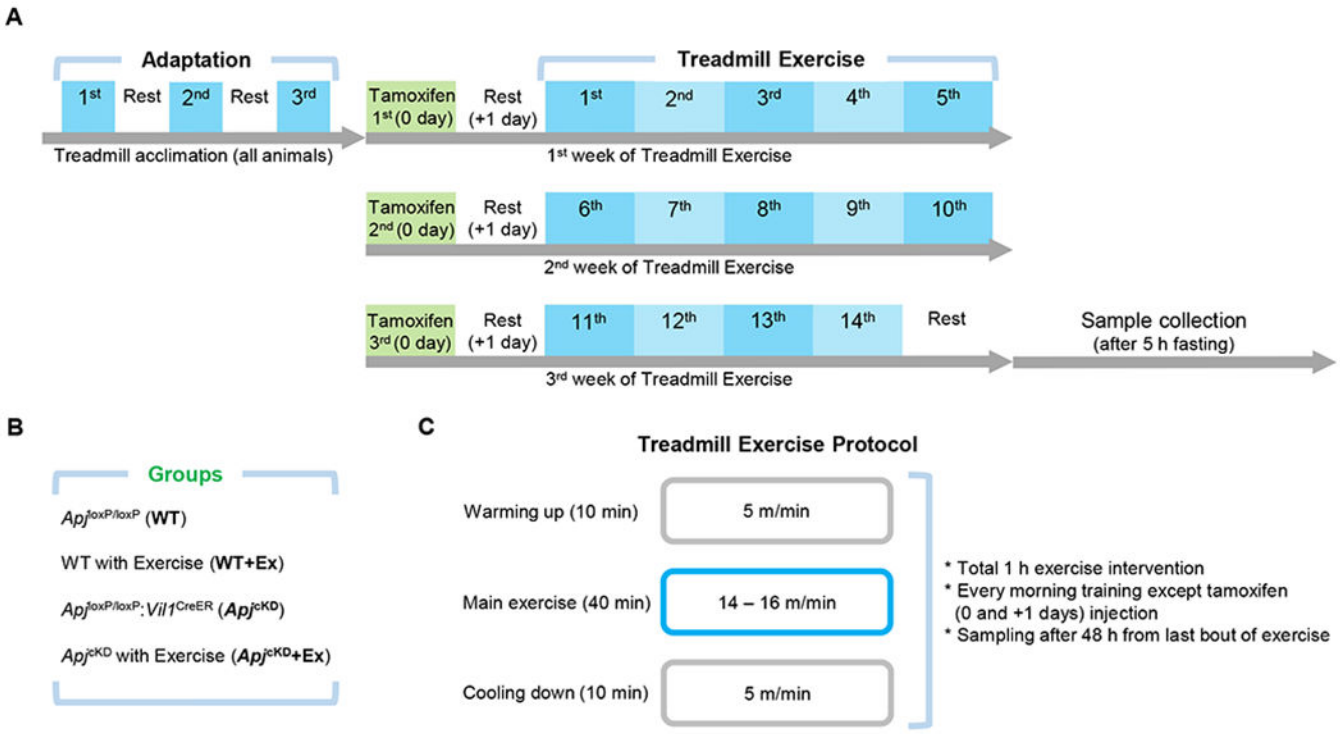

Figure 1. Study design and exercise training protocol.

(**A**) Arrangements of daily exercise, tamoxifen injection and necropsy in Flox-CreER mice. (**B**) Four groups utilized (n = 5/group). (**C**) Daily treadmill exercise regimen (speed and duration).

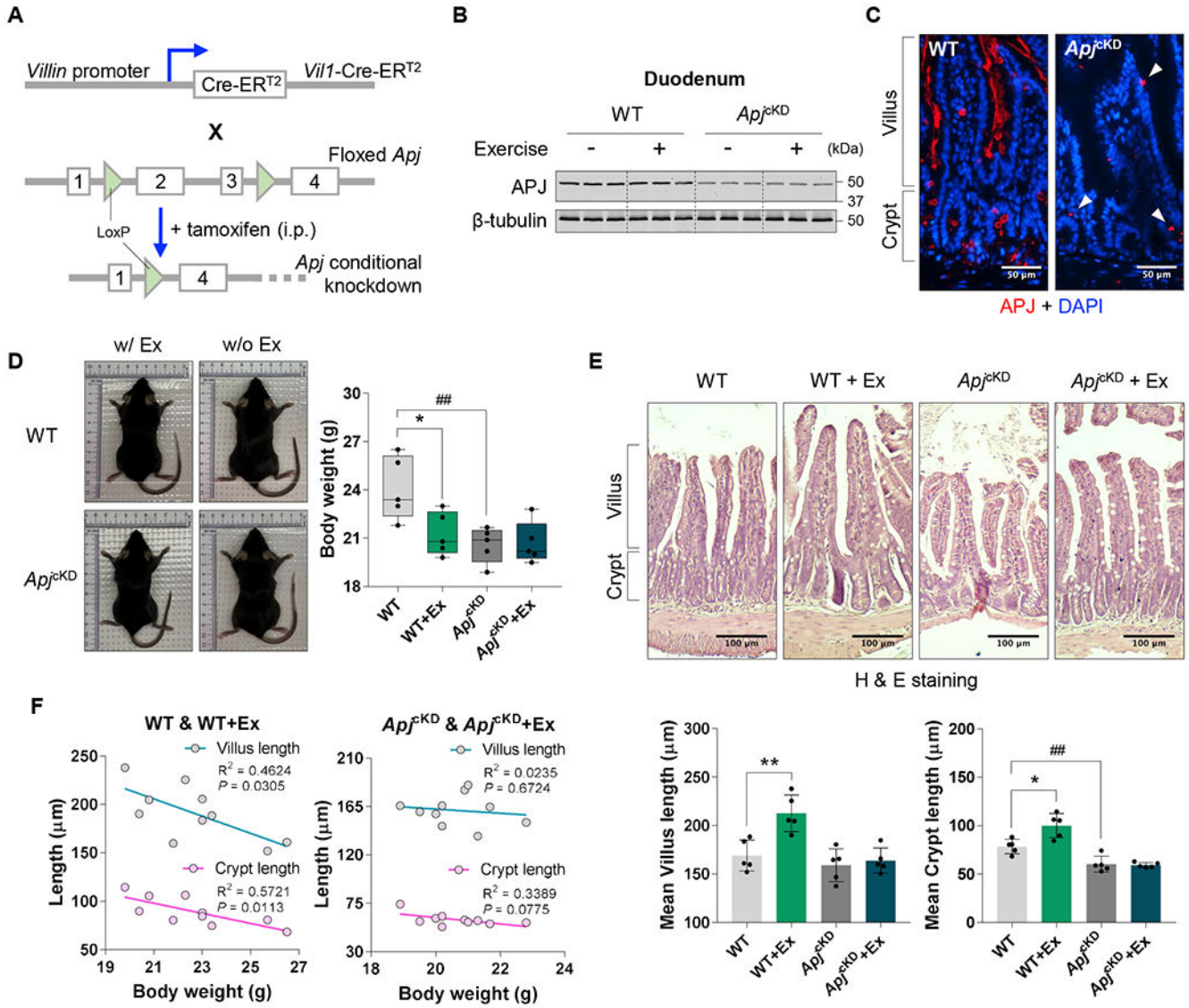

Figure 2. APJ is required for small intestine maintenance.

(**A**) A diagram showing transgenic mice with *Apj* floxed and *Villin* promoter driving the expression of the tamoxifen-dependent Cre-ER^{T2}. (**B,C**) Protein level of APJ (B) and immunocytochemical staining (C) of wild-type (WT; *Apj*$^{loxP/loxP}$) and *Apj* conditional knockdown (*Apj*^{cKD}; *Vil1*^{CreER};*Apj*$^{loxP/loxP}$) duodenum. (**D**) Representative body images (left) and means (right) following tamoxifen injection and exercise intervention (n = 5/group). (**E**) H&E staining of small intestine at 3 weeks post intervention (up) with quantification of villus and crypt length (down) (n = 5/group). (**F**) Pearson correlations of body weight with villus or crypt length in WT or *Apj* deleted mice. Data are presented as the mean ± SD, and each dot represents one litter. $^{*}P < 0.05$ and $^{**}P < 0.01$ in vs. Ex; $^{\#\#}P < 0.01$ in vs. *Apj*^{cKD} by two-way ANOVA followed by Tukey's test and unpaired Student's *t*-test (D,E) and Pearson correlation (F).

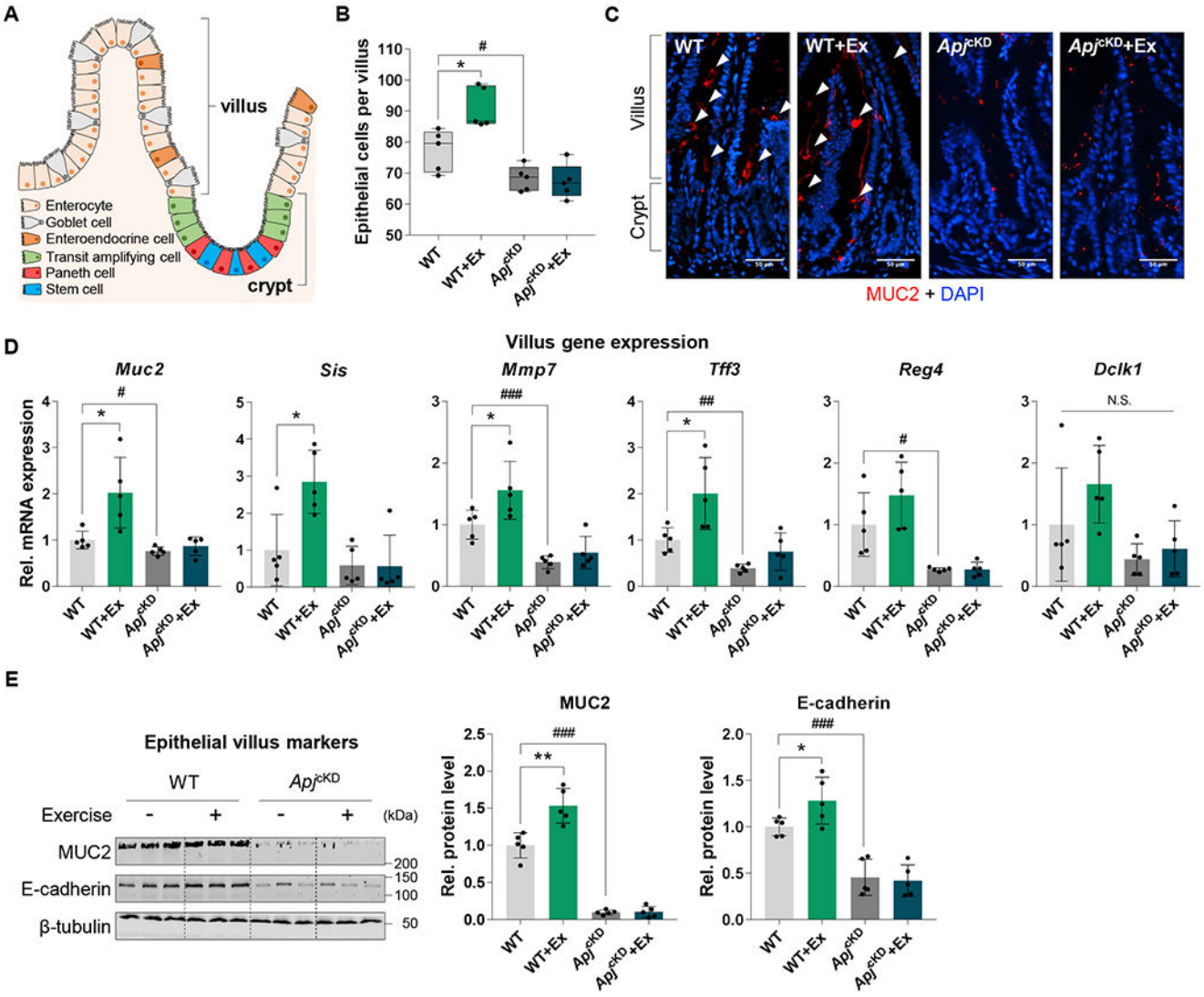

Figure 3. Exercise induces villus structure and remodeling via APJ.

(**A**) Schematic illustration of each cell in the villus and crypt. (**B**) Counts of epithelial cells per villus at post intervention (n = 5/group). (**C**) Representative immunocytochemical staining in villus and crypt at post intervention. Goblet cell marker (MUC2, red); DNA (DAPI, blue). Arrows indicate MUC2 positive cells. Scale bar = 50 μm. (**D**) mRNA expression of epithelial cell marker genes (*Muc2*, *Sis*, *Dclk2*) and secretory cell marker genes (*Mmp7*, *Tff3*, *Reg4*) (n = 5/group). (**E**) Cropped western blot images (left) and relative levels (right) of MUC2 and E-cadherin (β-tubulin were used for normalization; n = 5/group). Data are presented as the mean ± SD, and each dot represents one litter. $^{*}P < 0.05$ and $^{**}P < 0.01$ in vs. Ex; $^{\#}P < 0.05$, $^{\#\#}P < 0.01$, and $^{\#\#\#}P < 0.001$ in vs. *Apj*^{cKD} by two-way ANOVA followed by Tukey's test and unpaired Student's *t*-test (B-E).

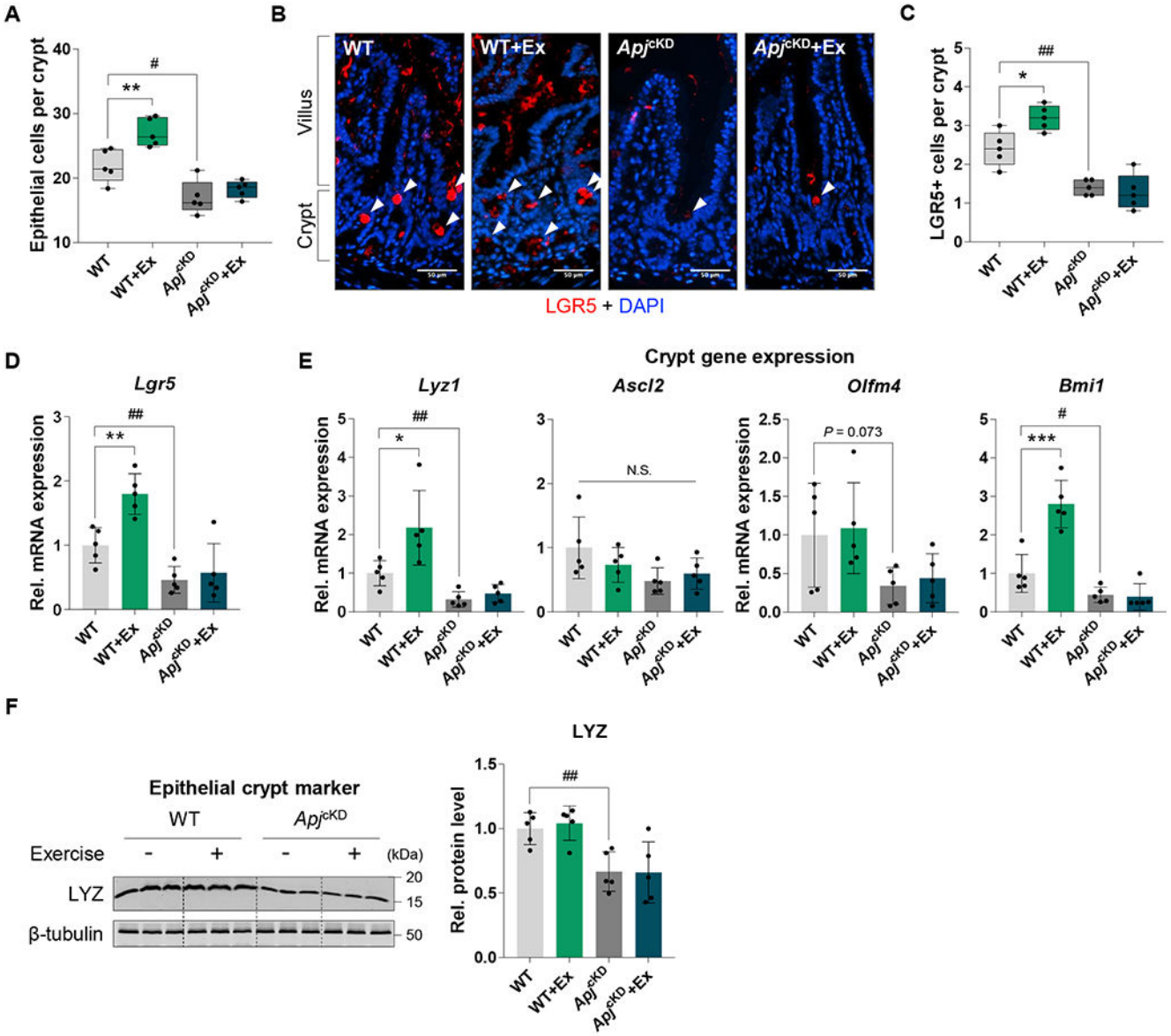

Figure 4. APJ is required for crypt remodeling in response to exercise intervention.

(**A**) Counts of epithelial cells per crypt at post intervention (n = 5/group). (**B,C**) Representative immunocytochemical staining in crypt (B) and counts of LGR5 positive cells per crypt (C) at post intervention (n = 5/group). Stem cell marker (LGR5, red); DNA (DAPI, blue). Arrows indicate LGR5 positive cells. Scale bar = 50 μm. (**D,E**) mRNA expression of *Lgr5* (D) and crypt marker genes (*Lyz1*, *Ascl2*, *Olfm4*, and *Bmi1*) (E) at post intervention (n = 5/group). (**F**) Cropped western blot images (left) and relative means (right) of LYZ at post intervention (β-tubulin was used for normalization; n = 5/group). Data are presented as the mean ± SD, and each dot represents one litter. $^{*}P < 0.05$, $^{**}P < 0.01$ and $^{***}P < 0.001$ in vs. Ex; $^{\#}P < 0.05$ and $^{\#\#}P < 0.01$ in vs. *Apj*^{cKD} by two-way ANOVA followed by Tukey's test and unpaired Student's *t*-test (A-F).

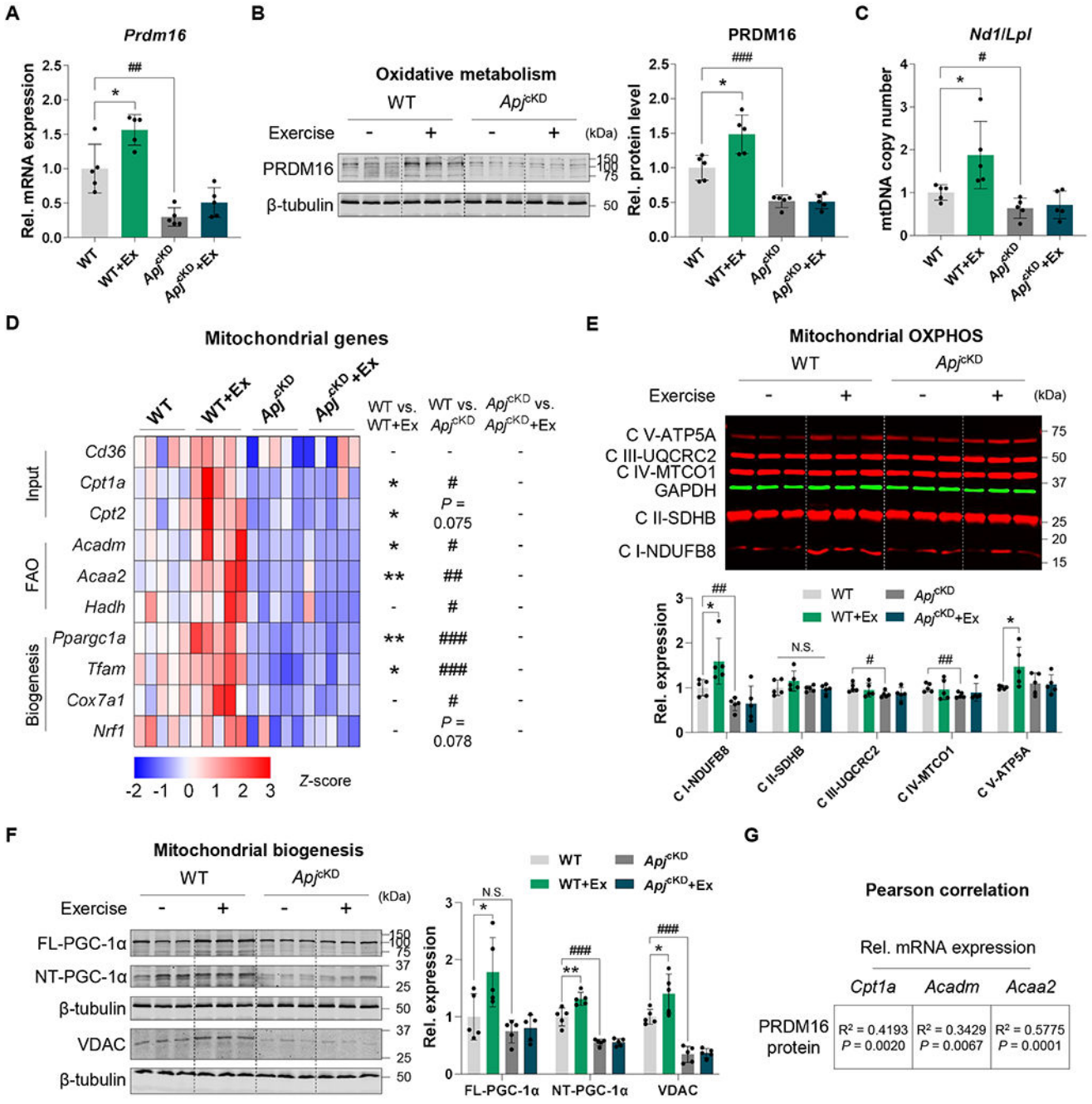

Figure 5. Exercise via APJ promotes the expression of fatty acid oxidation markers.

(**A,B**) mRNA expression (A) and cropped western blots (B) of PRDM16 at post intervention (n = 5/group). (**C**) Mitochondrial DNA copy number by mitochondrial DNA (*Nd1*) per genomic DNA (*Lpl*) at post intervention (n = 5/group). (**D**) mRNA expression of input genes (*Cd36*, *Cpt1a*, and *Cpt2*), mitochondrial fatty acid oxidation (FAO) genes (*Acadm*, *Acaa2*, and *Hadh*), and mitochondrial biogenic genes (*Ppargc1a*, *Tfam*, *Cox7a1*, and *Nrf1*) at post intervention (n = 5/group). (**E**) Cropped western blot images (up) and relative means (down) of OXPHOS at post intervention (GAPDH was used for normalization; n = 5/group).

(**F**) Cropped western blots of full length (FL) and truncated N-terminal (NT) isoforms of PGC-1α and VDAC at post intervention (β-tubulin was used for normalization; n = 5/group). (**G**) Pearson correlation between PRDM16 protein levels and the mitochondrial input gene (*Cpt1a*) or FAO gene (*Acadm* and *Acaa2*). Data are presented as the mean ± SD, and each dot represents one litter. $^{*}P < 0.05$ and $^{**}P < 0.01$ in vs. Ex; $^{\#}P < 0.05$, $^{\#\#}P < 0.01$, and $^{\#\#\#}P < 0.001$ in vs. Apf^{cKD} by two-way ANOVA followed by Tukey's test and unpaired Student's *t*-test (A-F) and Pearson correlation (G).

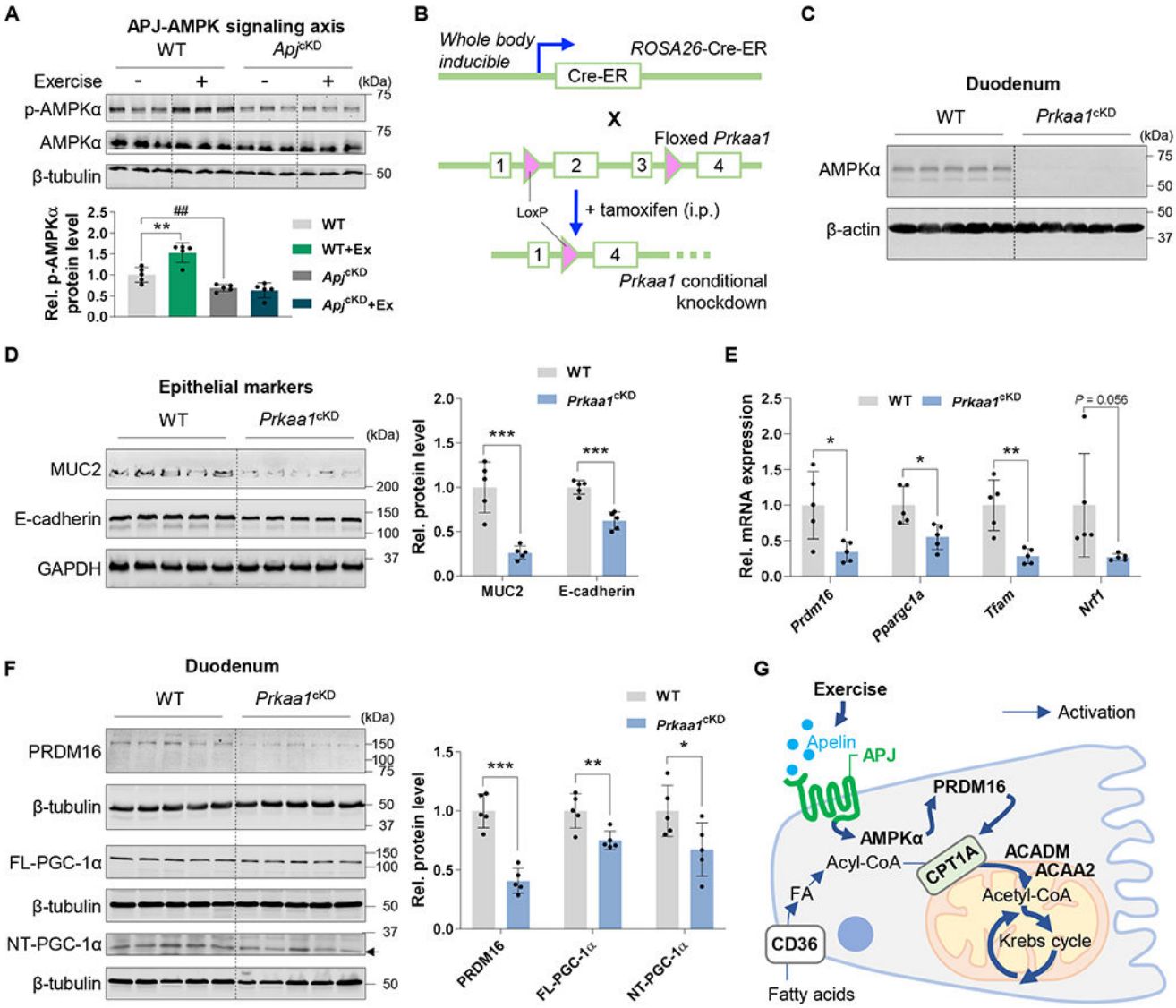

Figure 6. Exercise facilitates the intestinal epithelial homeostasis via APJ-AMPK axis.

(**A**) Cropped western blots of AMPK phosphorylation (A) and (β-tubulin was used for normalization; n = 5/group). (**B**) A diagram showing transgenic mice with *Prkaa1* floxed and *ROSA26-Cre-ER* driving the expression of the tamoxifen-dependent Cre-ER. (**C**) Protein level of AMPKα1 of wild-type (WT; *Prkaa1*$^{loxP/loxP}$) and *Prkaa1* conditional knockdown (*Prkaa1*^{cKD}; *ROSA26*^{CreER};*Prkaa1*$^{loxP/loxP}$) mice. (**D**) Cropped western blots and means of MUC2 and E-cadherin in WT and *Prkaa1*^{cKD}duodenum (GAPDH was used for normalization; n = 5/group). (**E**) mRNA expression of *Prdm16* and mitochondrial biogenesis marker genes, *Ppargc1a*, *Tfam*, and *Nrf1* in AMPKα1 deleted duodenum (n = 5). (**F**) Cropped western blots of PRDM16 and full length (FL) and truncated N-terminal (NT) isoforms of PGC-1α in AMPKα1 deleted duodenum (β-tubulin was used for normalization; n = 5). (**G**) A schematic diagram suggesting that exercise enhances PRDM16 and its downstream FAO via APJ-AMPK. Data are presented as the mean ± SD, and each dot

represents one litter. $^{*}P < 0.05$, $^{**}P < 0.01$, and $^{***}P < 0.001$ in vs. Ex or *Prkaa1*^{cKD}; $^{\#\#}P < 0.01$ in vs. *Apj*^{cKD} by two-way ANOVA followed by Tukey's test (A) and unpaired Student's *t*-test (A-F).

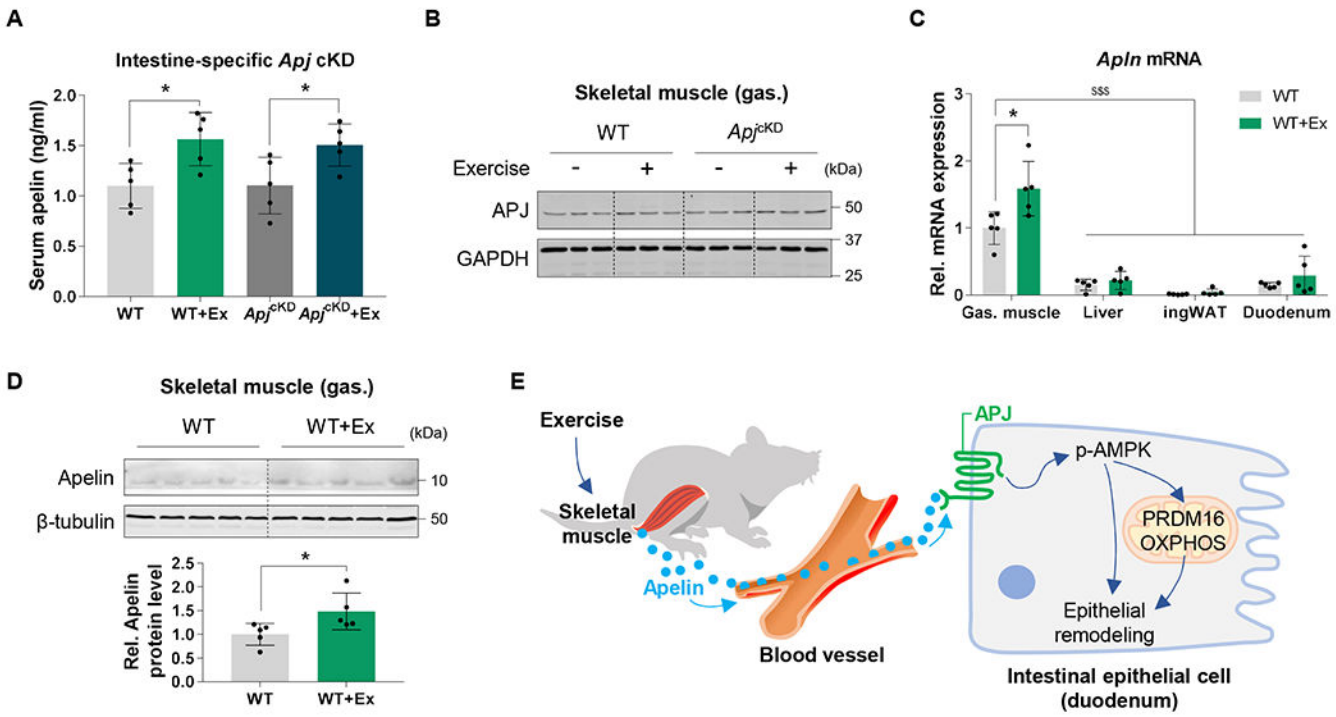

Figure 7. Exercise increases skeletal muscle apelin secretion to regulate intestinal remodeling.

(**A**) Serum apelin concentration via EIA kit in intestine-specific wild-type (WT; $Apj^{loxP/loxP}$) and *Apj* conditional knockdown (Apj^{cKD}; $Vil1^{CreER}$;$Apj^{loxP/loxP}$) (n = 5/group). (**B**) Gastrocnemius muscle APJ protein levels in intestine-specific wild-type (WT; $Apj^{loxP/loxP}$) and *Apj* conditional knockdown (Apj^{cKD}; $Vil1^{CreER}$;$Apj^{loxP/loxP}$). (**C**) *Apln* mRNA expression in gastrocnemius (Gas.) muscle, liver, inguinal white adipose tissue (ingWAT), and intestinal duodenum at post intervention (n = 5/group). (**D**) Cropped western blots of apelin in the Gas. muscle at post intervention (β-tubulin was used for normalization; n = 5/group). (**E**) Suggested schematic mechanisms: exercise induces apelin expression in muscle which releases into the circulation to activate APJ-AMPK axis and facilitate intestinal epithelial remodeling. Data are presented as the mean ± SD, and each dot represents one litter. $*P < 0.05$ in vs. Ex by two-way ANOVA followed by Tukey's test (A) and unpaired Student's *t*-test (C,D).

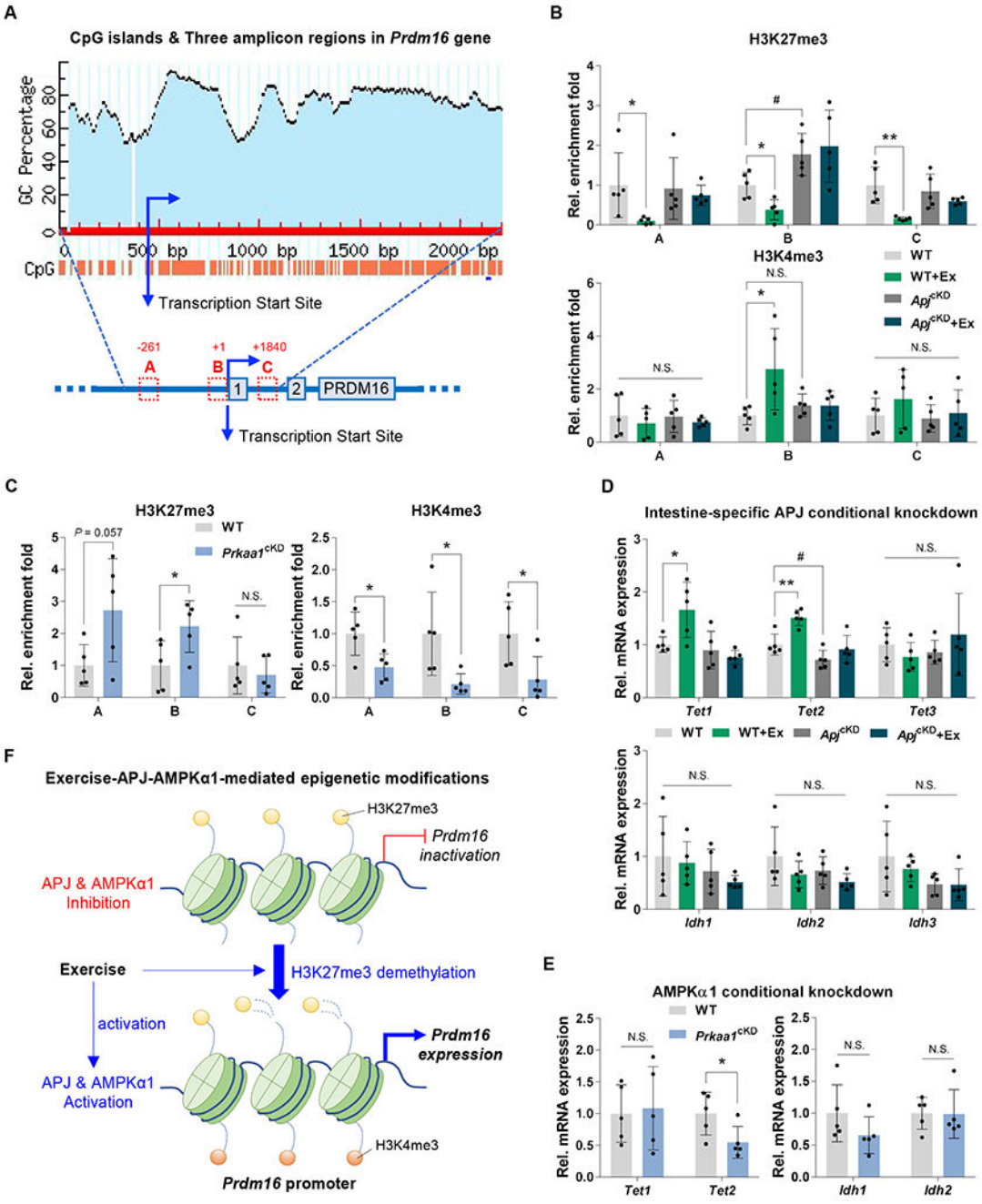

Figure 8. Exercise-induced histone modifications facilitate *Prdm16* expression via APJ-AMPK axis.

(**A**) Location of CpG islands for histone modifications in the *Prdm16* promoter based on our previous study (Yang et al., 2016b) by MethPrimer (Li & Dahiya, 2002). (**B**) H3K27me3 and H3K4me3 modifications in the *Prdm16* promoter of WT and intestine-specific APJ KD with/without exercise (n = 5). (**C**) H3K27me3 and H3K4me3 modifications in the *Prdm16* promoter of WT and AMPKα1 KD (n = 5). (**D**,**E**) mRNA expression of TET family, *Tet1*, *Tet2*, and *Tet3*, and IDH family, *Idh1*, *Idh2*, and *Idh3*, in intestine-specific APJ deleted

duodenum (D; n = 5) and AMPKα1 deleted duodenum (E; n = 5). (**F**) A proposed diagram for the effects of exercise on histone modifications in the *Prdm16* promoter by APJ-AMPK axis. Data are presented as the mean ± SD, and each dot represents one litter. $*P < 0.05$ and $**P < 0.01$ in vs. Ex or $Prkaa1^{cKD}$; $^{\#}P < 0.05$ in vs. Apj^{cKD} by two-way ANOVA followed by Tukey's test (B, D) and unpaired Student's *t*-test (B-E).

Table 1.

Primer sequences used for qPCR analysis.

Gene Name	Forward/Reverse	Primer sequence
Lyz1	F	5’-GGAATGGATGGCTACCGTGG-3’
	R	5’-CATGCCACCCATGCTCGAAT-3’
Lgr5	F	5’-TAAAGACGACGGCAACAGTG-3’
	R	5’-GCCTTCAGGTCTTCCTCAAA-3’
Ascl2	F	5’-TGCCAGAGCTGATTGACATTC-3’
	R	5’-GGCATACCAGAAGGTGGTGAG-3’
Olfm4	F	5’-TGAAGGAGATGCAAAAACTGG-3’
	R	5’-CTCCAGCTTCTCTACCAAGAGG-3’
Bmi1	F	5’-TTCATTGTCTTTTCCGCCCG-3’
	R	5’-AGTACCCTCCACACAGGACA-3’
Muc2	F	5’-TCCTGACCAAGAGCGAACAC-3’
	R	5’-ACAGCACGACAGTCTTCAGG-3’
Sis	F	5’-CGTTTCCGGTTCAAGCTCACA-3’
	R	5’-CCTGATGACTTTGATGCTGAACG-3’
Mmp7	F	5’-AGGAAGCTGGAGATGTGAGC-3’
	R	5’-TCTGCATTTCCTTGAGGTTG-3’
Tff3	F	5’-TTGCTGGGTCCTCTGGGATAG -3’
	R	5’-TACACTGCTCCGATGTGACAG-3’
Reg4	F	5’-CTGAGCTGGAGTGTCAGTCAT-3’
	R	5’-GTCCACTGCCATAATTGCTTCT-3’
Dclk1	F	5’-GGGTGAGAACCATCTACACCATC-3’
	R	5’-CCAGCTTCTTAAAGGGCTCGAT-3’
Prdm16	F	5’-TGTGCGAAGGTGTCCAAACT-3’
	R	5’-AACGTCACCGTCACTTTTGG-3’
Ppargc1a	F	5’-CCATACACAACCGCAGTCGC-3’
	R	5’-GTGGGAGGAGTTAGGCCTGC-3’
Tfam	F	5’-CCAAAAAGACCTCGTTCAGC-3’
	R	5’-CTTCAGCCATCTGCTCTTCC-3’
Cox7a1	F	5’-CAGCGTCATGGTCAGTCTGT-3’
	R	5’-AGAAAACCGTGTGGCAGAGA-3’
Nrf1	F	5’-GCACCTTTGGAGAATGTGGT-3’
	R	5’-CTGAGCCTGGGTCATTTTGT-3’
Cpt1a	F	5’-TCGCTCATTCCGCCGC-3’
	R	5’-GAGATCGATGCCATCAGGGG-3’
Cpt2	F	5’-TTCTGCAGTGCGGTTTCTGA-3’
	R	5’-GTGTCACTTCTGGCAGGGTT-3’
Acadm	F	5’-AGGGTTTAGTTTTGAGTTGACGG-3’
	R	5’-CCCCGCTTTTGTCATATTCCG-3’
Cd36	F	5’-TGAATGGTTGAGACCCCGTG-3’

Gene Name	Forward/Reverse	Primer sequence
	R	5’-TAGAACAGCTTGCTTGCCCA-3’
Acaa2	F	5’-GAACGAAGCTTTTGCCCCTC-3’
	R	5’-CTTTCCACCTCGACGCCTTA-3’
Hadh	F	5’-CCATCTTTGCCAGCAACACG-3’
	R	5’-GCACGGGGTTGAAAAAGTGG-3’
Apln	F	5’-GTTTGTGGAGTGCCACTG-3’
	R	5’-CGAAGTTCTGGGCTTCAC-3’
Tet1	F	5’-CACCCTGTGACTGTGATGGAGGTA-3’
	R	5’-ACTATCTTCTCAATCCGGATTGCCTT-3’
Tet2	F	5’-AAGGATGCAATCCAGACAAAGATGAA-3’
	R	5’-TTTAGCAATAGGACATCCCTGAGAGCT-3’
Tet3	F	5’-GAACTCATGGAGGATCGGTATGGA-3’
	R	5’-CAGCTTCTCCTCCAGTGTGTGTCTT-3’
Idh1	F	5’-ACATGCATATGGGGACCAATACAGA-3’
	R	5’-TTCAAAGTCATGTACCATGTATGTCACC-3’
Idh2	F	5’-GCAGTTCATCAAGGAGAAGCTCATC-3’
	R	5’-CACACTTGACAGCCACACTGTACTTCT-3’
Idh3	F	5’-TCAAGGAAGTGTTCAAGGCTGCTG-3’
	R	5’-GATGGCAACTTTGTTCTCCTTCATG-3’
Prdm16 ChIP A	F	5’-AGAGAGAAGTGAGGTGAAGACCGAGAA-3’
	R	5’-ACACACTATCTTCATCTCCCTAGCATTGT-3’
Prdm16 ChIP B	F	5’-GCATGTGCGAAGGTGTCCAAA-3’
	R	5’-TGGATCGCATGGTGTCGGCT-3’
Prdm16 ChIP C	F	5’-CCAAAGCTTGAAGGAGAGAGACGTAAA-3’
	R	5’-TCGGTTCTTGGCCTCCAGAGAAG-3’
18S	F	5’-GTAACCCGTTGAACCCCATT-3’
	R	5’-CCATCCAATCGGTAGTAGCG-3’